Cyclic distension of fibrin-based tissue constructs: Evidence of adaptation during growth of engineered connective tissue

Zeeshan H. Syedain*, Justin S. Weinberg†, and Robert T. Tranquillo*†‡

Departments of *Chemical Engineering and Materials Science and †Biomedical Engineering, University of Minnesota, Minneapolis, MN 55455

Edited by Robert Langer, Massachusetts Institute of Technology, Cambridge, MA, and approved March 11, 2008 (received for review November 29, 2007)

Tissue engineering provides a means to create functional living tissue replacements. Here, we examine the effects of 3 weeks of cyclic distension (CD) on fibrin-based tubular tissue constructs seeded with porcine valve interstitial cells. CD with circumferential strain amplitude ranging from 2.5% to 20% was applied to evaluate the effects of CD on fibrin remodeling into tissue. We hypothesized that during long-term CD cells adapt to cyclic strain of constant strain amplitude (constant CD), diminishing tissue growth. We thus also subjected constructs to CD with strain amplitude that was incremented from 5% to 15% over the 3 weeks of CD [incremental CD (ICD)]. For constant CD, improvement occurred in construct mechanical properties and composition, peaking at 15% strain: ultimate tensile strength (UTS) and tensile modulus increased 47% and 45%, respectively, over statically incubated controls (to 1.1 and 4.7 MPa, respectively); collagen density increased 29% compared with controls (to 27 mg/ml). ICD further improved outcomes. UTS increased 98% and modulus increased 62% compared with the largest values with constant CD, and collagen density increased 34%. Only in the case of ICD was the ratio of collagen content to cell number greater (70%) than controls, consistent with increased collagen deposition per cell. Studies with human dermal fibroblasts showed similar improvements, generalizing the findings, and revealed a 255% increase in extracellular signal-regulated kinase signaling for ICD vs. constant CD. These results suggest cell adaptation may limit conventional strategies of stretching with constant strain amplitude and that new approaches might optimize bioreactor operation.

ERK signal | tissue engineering | valve interstitial cells | dermal fibroblast | mechanical loading | conditioning

The vast majority of approaches to cardiovascular tissue engineering involve seeding matrix-producing cells, typically smooth muscle cells, fibroblasts, and/or myofibroblasts, onto a synthetic polymer or entrapping the cells within a forming biopolymer gel cast in a mold. In either case, there is typically an *in vitro* culture stage with the goal of having the cells transform the starting polymer into tissue that confers the required properties of the tissue-engineered construct. Essential criteria for a successful construct in many applications include requisite mechanical properties such as sufficient tensile and/or burst strength, physiological modulus/compliance, and elastic recoil. This endeavor has been coined "functional tissue engineering" (1). Achieving these properties has motivated several strategies and bioreactor concepts, including the use of chemical stimulation (e.g., growth factor supplementation to the construct incubation medium) and mechanical stimulation (e.g., stretching, compressing, or bending the construct). Mechanical stimulation has become a primary strategy for inducing tissue growth *in vitro* (2).

In vascular tissue engineering, cyclic distension (CD) of constructs via pulsatile flow of medium through the lumen (3–5) or inflation of an elastic tube placed through the lumen (6–9) are the primary bioreactor configurations. In particular, mechanical properties of tissue constructs have been shown to improve when stretching constructs prepared by seeding cells on synthetic polymers (10, 11) and entrapping cells in collagen (7, 9). A recent review of related research is available (12).

In heart valve tissue engineering, CD/stretching of constructs has been accomplished by pulsatile flow of medium through the valve (13, 14) or pulsatile back-pressure on the valve (15). The cell types primarily investigated in these studies have been dermal and adventitial fibroblasts and valve interstitial cells (VICs), which are predominantly a myofibroblast phenotype (16). As with vessel constructs, mechanical properties of valve constructs have been shown to improve with cyclic stretching and correlate with ECM deposition and cell proliferation (15, 17).

We use fibrin gel as the scaffold for fabrication of bioartificial arteries and heart valves because it is conducive to collagen deposition under static culture conditions (18). However, we have not yet assessed the outcome of using fibrin in a bioreactor designed to impart mechanical stretching. In this study we assessed the outcome of CD during culture of tubular fibrin constructs with entrapped tissue cells, which has relevance to the design and operation of bioreactors to cyclically stretch fibrin-based valve constructs (19) and fibrin-based artery constructs (20). We have previously shown that fibroblasts and VICs remodel fibrin disk-shaped constructs adherent to tissue culture plastic (21). Although a static tension develops in these constructs, which is likely an important stimulatory signal (22), it is not a cyclic tension as occurs during cyclic stretching.

The vast majority of studies that have examined the effects of CD on tubular constructs have restricted their conditions to CD with constant parameters, specifically strain amplitude, stretch time, and relaxation time (the last two being equivalent to frequency and duty cycle). However, it is well known that cells adapt their behavior to constant environmental stimuli; that is, cells initially respond but return to a baseline level after sustained stimulation (23–25). A well known and relevant example of adaptation exhibited by mammalian cells is the response of osteoblasts to mechanical loading (25–27). Schriefer *et al.* (26) studied this in rat ulnar bone and found significantly higher bone mineral content with an applied cyclic loading, but with the mineralization diminishing over time. Kim *et al.* (27) observed significant trabecular bone formation occurring in response to loading within the first week, with significantly less during weeks 2–4 of loading.

To understand how bone tissue responds to changing environment, Tang *et al.* (28) examined the effects of stepwise

Author contributions: Z.H.S. and R.T.T. designed research; Z.H.S. and J.S.W. performed research; Z.H.S., J.S.W., and R.T.T. contributed new reagents/analytic tools; Z.H.S., J.S.W., and R.T.T. analyzed data; and Z.H.S. and R.T.T. wrote the paper.

The authors declare no conflict of interest.

This article is a PNAS Direct Submission.

‡To whom correspondence should be addressed. E-mail: tranquillo@cems.umn.edu.

This article contains supporting information online at www.pnas.org/cgi/content/full/0711217105/DCSupplemental.

increasing strain amplitude on cyclic stretch of osteoblasts cultured on a distensible substratum. In that study, the higher-strain amplitude steps were correlated with diminishing collagen production by the cells; hence, no overall significant benefit of using stepwise incremental strain amplitude during cyclic stretching was found. (The incubation times used in that study were at most 24 h compared with the weeks needed to achieve significant tissue growth *in vitro*. Also, the applied strain levels used were physiologically relevant for osteoblasts but an order of magnitude below those typically used in cardiovascular tissue engineering, and the cells were not entrapped in a 3D polymeric scaffold.)

Thus, in this study, we also examined the effect of periodically changing the CD strain amplitude in stepwise increments in addition to using constant strain amplitude, the latter being the conventional approach, to assess whether adaptation may play a role in the success of using long-term CD to achieve tissue growth. Samples were characterized in terms of mechanical properties, collagen content, cellularity, and histology to elucidate the basis for any improvement in mechanical properties caused by CD. Selected samples were also assayed for activation of the extracellular signal-regulated kinase (ERK) signaling pathway, which has been correlated to collagen expression during mechanical stretching of fibroblasts on a distensible membrane (29), to establish a mechanistic basis for any adaptation.

Results

Tubular constructs were cultured for 3 weeks on a distensible latex mandrel in the CD bioreactor, during which time no downward movement was observed. Upon harvest, all constructs slid off the mandrel, indicating there was insignificant adhesion to the latex mandrel and that construct elasticity maintained it in contact with the latex mandrel during CD. Unless indicated, all results were derived from constructs prepared with porcine VICs (PVICs). For brevity, constant strain amplitude CD and stepwise incremental strain amplitude CD experiments are referred to as simply "CD" and "ICD," respectively, and paired statically incubated controls are referred to as "controls."

CD and ICD Results in Different Construct Dimensions but Not Different Volumes. As seen in supporting information (SI) Fig. S1, the final length and thickness inversely varied with some conditions; however, all constructs were <1% of their initial volume, with no difference between the final volumes of the CD and ICD constructs and their controls.

CD Improves Construct Mechanical Properties. Fig. 1 shows there was no improvement in mechanical properties for 2.5% and 5% CD, but improvements in ultimate tensile strength (UTS) and tensile modulus (E) were observed for 10% and 15% CD. At 10%, the UTS increased 29% compared with controls and E increased 59% compared with controls. At 15% CD, UTS increased 47% compared with controls, and E increased 45% compared with controls. Absolute values of UTS and E are presented in Table 1. Further studies were conducted at 20% CD; however, the majority of the constructs either tore during the first week of CD or were permanently deformed (slid down the mandrel), indicating a strain amplitude between 15% and 20% causes damage to the growing tissue in this system.

Fig. 2*a* shows there was no increase in collagen concentration at 2.5%, 5%, or 10% CD. At 15%, the collagen concentration increased 29% compared with controls. There was no difference in the cell concentration at 2.5%, 5%, or 10% (Fig. 2*b*); however, at 15% it increased by 47% compared with controls. For the collagen concentration normalized by the cell concentration, a measure of the collagen deposited in the ECM per cell, there was no difference between CD constructs and controls (Fig. 2*c*).

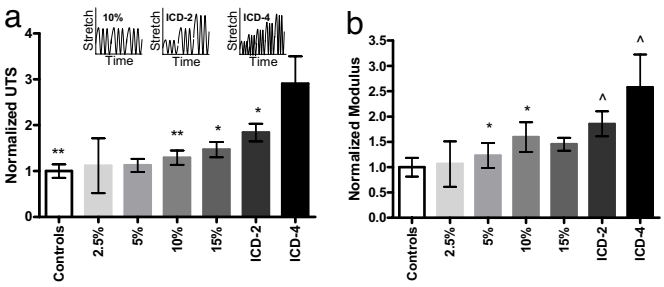

Fig. 1. Tensile mechanical properties of constructs after CD. (*a*) Normalized UTS. (*b*) Normalized modulus (E). Values are normalized to paired static controls. In all cases where error bars are not overlapping, the means are significantly different ($P < 0.05$); for groups with overlapping error bars, a significant difference ($P < 0.05$) between means is shown with paired symbols. (*Inset*) Schematic of CD and ICD regimens: CD, shown for 10% strain amplitude, ICD with two steps (ICD-2), the amplitude changed from 5% → 10% → 15%, and ICD with four steps (ICD-4), the amplitude changed from 5% → 7.5% → 10% → 12.5% → 15%.

Absolute values of cell and collagen concentrations and their ratios are presented in Table 2.

ICD Further Improves Construct Mechanical Properties and Correlates with Increased Net Collagen Deposition per Cell. Constructs were subjected to ICD from 5% to 15% in two (ICD-2) and four (ICD-4) equal time steps over 3 weeks (Fig. 1). For ICD-2, UTS increased by 84% and E increased by 85% compared with controls. ICD-4 further improved the mechanical properties, with UTS increased by 191% and E increased by 158% compared with controls. Comparing the highest UTS and E achieved with CD, the UTS was 98% higher with ICD-4 in comparison with 15% CD, and E was 61% higher with ICD-4 in comparison with 10% CD.

Collagen concentration increased 55% for ICD-2 and 73% for ICD-4 compared with controls as shown in Fig. 2*a*. The collagen concentration was 34% higher with ICD-4 in comparison with 15% CD, which had the highest value among all CD groups. There was no difference in cell concentration for ICD-2 or ICD-4 compared with controls. However, the collagen concentration normalized by the cell concentration was greater than controls for both ICD-2 (by 37%) and ICD-4 (by 70%).

ICD Yields Similar Results for Human Dermal Fibroblast (HDF)-Populated Constructs. Similar to PVIC constructs, constructs prepared from neonatal HDFs showed improved mechanical properties and collagen concentration with both CD and ICD compared

Table 1. UTS and modulus (E) of constructs subjected to CD paired static controls

Construct/control	UTS ± SD, kPa	Modulus ± SD, kPa
2.5% CD	1,188 ± 637	5,610 ± 2,364
2.5% controls	1,064 ± 272	5,280 ± 884
5% CD	758 ± 68	4,478 ± 896
5% controls	673 ± 103	3,638 ± 541
10% CD	923 ± 113*	5,267 ± 972*
10% controls	714 ± 66	3,302 ± 417
15% CD	1,112 ± 126*	4,706 ± 416*
15% controls	758 ± 228	3,235 ± 894
ICD-2	2,500 ± 261*	12,733 ± 1,698*
ICD-2 controls	1,359 ± 190	6,865 ± 906
ICD-4	2,295 ± 467*	11,407 ± 2,867*
ICD-4 controls	789 ± 408	4,428 ± 2,339

*Significant difference ($P < 0.05$) between CD and paired static controls.

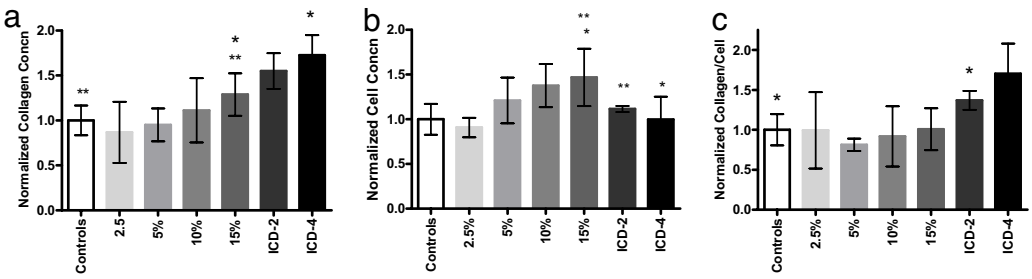

Fig. 2. Composition of PVIC constructs after CD. (*a*) Normalized collagen concentration. (*b*) Normalized cell concentration. (*c*) Normalized collagen concentration/cell concentration. See Fig. 1 regarding statistical significance.

with controls. With 10% CD, UTS increased 85% compared with controls (903 ± 126 kPa vs. 489 ± 50 kPa) and E increased 127% compared with controls (3160 ± 416 kPa vs.1392 ± 138 kPa). With ICD-4, UTS increased 61% (to 1453 ± 102 kPa) and E increased 36% (to 4306 ± 189 kPa) compared with 10% CD. In comparison to controls, UTS increased 197% and E increased 209%. The collagen concentration increased 84% (to 24 ± 3 mg/cm^3) with 10% CD and 178% (to 36 ± 1 mg/cm^3) with ICD-4 compared with controls.

CD-Mediated Improvement in Tissue Growth Requires 2–3 Weeks of CD. To elucidate whether a critical period for tissue development existed, HDF constructs were characterized just before CD at week 2 and then weekly for the 3-week CD period. The time-course data for HDF constructs shown in Fig. 3 reveal the increases in UTS (Fig. 3*a*) and collagen content (Fig. 3*b*) caused by 10% CD and ICD-4 occurred largely during the third week of CD. For the ICD-4 case, the UTS increased 52% during week 2 and 197% during week 3 compared with controls.

CD Results in Collagen Maturation in Constructs. Using Picrosirius red staining, we examined collagen maturation in histological cross-sections of constructs. As shown in Fig. 4, there was stronger staining in CD and ICD constructs (*k*, *l*, and *s*–*u*) compared with controls (*j* and *r*), suggesting that CD and ICD induced collagen maturation, which contributed to the improved mechanical properties. It can be further observed that staining was brighter in ICD constructs (Fig. 4 *l*, *t*, and *u*) compared with CD constructs (Fig. 4 *k* and *s*). Based on the Trichrome-stained sections, the cells appear more strongly aligned in the circumferential direction in CD and ICD constructs (Fig. 4 *e*, *f*, and *n*–*p*) compared with controls (Fig. 4 *d* and *m*), indicating that CD and ICD induced cell and collagen alignment.

ICD Results in Elevated ERK 1/2 Signaling. To investigate the mechanism for improved tissue growth with ICD and develop evidence to test the adaptation hypothesis, we measured the activation of ERK (Fig. 5). In the case of ICD-4, this measurement corresponded to 4 days after the final increment in strain amplitude. Whereas total ERK was similar for 10% CD, ICD-4, and controls, the fraction of ERK that was phosphorylated ERK (pERK) after 3 weeks of CD was 255% greater for ICD vs. CD.

Table 2. Collagen concentration, cell concentration, and collagen per cell in constructs subjected to CD with paired static controls

Construct/ control	Collagen ± SD, mg/ml	Cell ± SD, million cells/ml	Collagen/cell ± SD, ng/cell
2.5% CD	22.2 ± 8.7	220 ± 65	0.11 ± 0.05
2.5% controls	25.6 ± 1.8	243 ± 30	0.11 ± 0.02
5% CD	15.6 ± 3.0	131 ± 28	0.12 ± 0.01
5% controls	16.4 ± 4.8	109 ± 21	0.15 ± 0.03
10% CD	18.2 ± 5.9	133 ± 21	0.14 ± 0.06
10% controls	16.4 ± 4.8	102 ± 21	0.15 ± 0.03
15% CD	27.4 ± 5.0*	308 ± 66*	0.09 ± 0.02
15% controls	21.3 ± 2.6	210 ± 77	0.11 ± 0.02
ICD-2	46.6 ± 5.9*	290 ± 21	0.16 ± 0.01*
ICD-2 controls	30.1 ± 2.3	260 ± 47	0.12 ± 0.02
ICD-4	41.3 ± 5.3*	204 ± 70	0.21 ± 0.05*
ICD-4 controls	23.9 ± 5.3	211 ± 39	0.12 ± 0.02

*Significant difference ($P < 0.05$) between CD and paired static controls.

Discussion

This study showed that CD can be used to improve the mechanical properties of cell-seeded fibrin-based tubular constructs. The study also revealed an apparent adaptation of the cells to long-term CD. With ICD, the UTS increased ≈300% compared with static culture, as compared with a modest 50% increase for constant CD. pERK also was elevated for ICD relative to CD, consistent with ICD overcoming a tendency of cells to adapt to CD. Histological analysis showed maximal alignment and maturation of collagen in the case of ICD.

Several studies have investigated the effect of CD on tissue-engineered tubular constructs (5, 9, 11). However, most studies have been limited to a single distension condition or short durations. In short durations, cell-induced gel compaction alone, causing a structural remodeling of the gel, can have a significant influence on the mechanical properties of collagen and fibrin gels before any significant compositional remodeling occurs. Furthermore, in the case of fibrin, rapid fibrinolysis can occur over short durations, if not controlled as done in this study with the inhibitor aminocaproic acid with PVIC constructs; the "compaction" may thus reflect fibril degradation and consolidation. To isolate the effects of CD on construct properties without the influence of extensive fibrin compaction, we incubated fibrin-based tubular constructs for 2 weeks on their mandrels in static culture before mounting them in the CD bioreactor. This allowed almost all of the volume reduction (exceeding 95%) to occur before the CD initiated at week 2, in

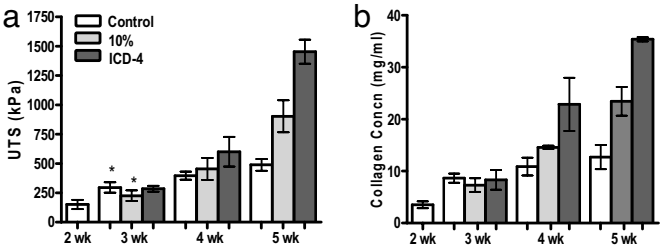

Fig. 3. Time course of HDF constructs during CD. (*a*) UTS. (*b*) Collagen concentration. See Fig. 1 regarding statistical significance.

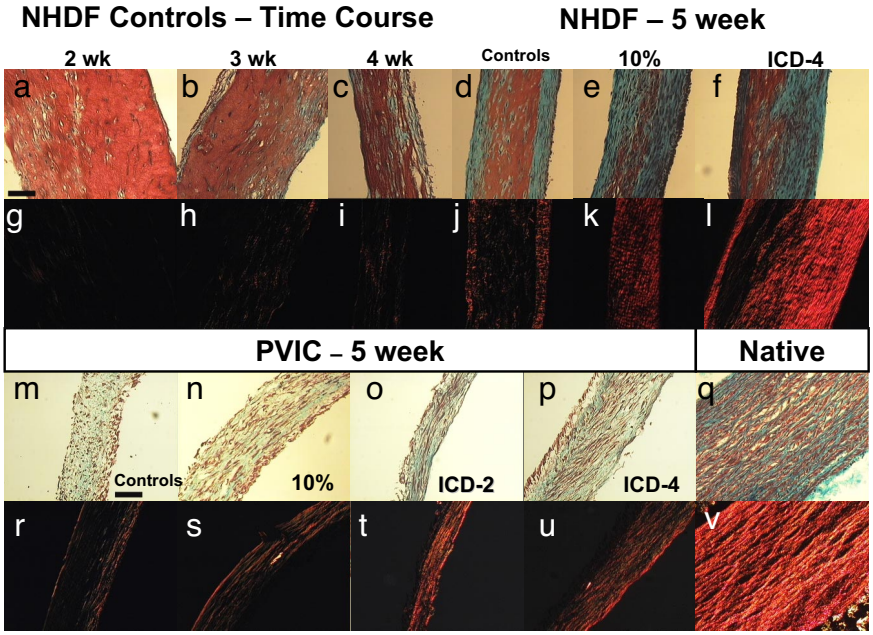

Fig. 4. Histology of constructs after CD. Lillie's Trichrome-stained sections of static control samples (*a–d* and *m*) for corresponding CD samples (*e*, *f*, and *n–p*) and Picrosirius red-stained sections for static control samples (*g–j* and *r*) for corresponding CD samples (*k*, *l*, and *s–u*). For comparison, stained sections of porcine carotid artery, Trichrome (*q*) and Picrosirius red (*v*) are also shown. All images were acquired at the same magnification. (Scale bars: 100 μm.)

comparison to that occurring over the 3-week CD period (an additional 4%, to 99% total). In the 5% CD constructs, more axial shortening occurred than in controls, but there was no improvement in mechanical properties, indicating that any effect of CD on length or thickness occurring in these experiments had no correlation with construct mechanical properties; moreover, these variations in length and thickness were offsetting in that there were no differences in volume reduction between CD constructs and controls (Fig. S1).

Several studies using both cells on membranes and cells in 3D scaffolds have shown increased cell-produced ECM when cells are subjected to cyclic stretching. *In vivo*, VIC are subject to large strain values during each cardiac valve cycle; Lo and Vesely (30) reported a maximum stretch of 24% in the radial direction and 11% in the circumferential direction. *In vitro*, using PVIC cultured on a flexible membrane, Ku *et al.* (31) have shown improved incorporation of [^{3}H]proline (indicative of higher collagen production) when subjected to 10%, 14%, and 20% CD. In the current study, using PVIC in fibrin-based tubular constructs subjected to CD, we found no improvement in either mechanical properties or collagen concentration at low strain amplitudes (2.5% and 5%), which suggests that there is a strain threshold below which cells have no apparent response to CD. Similar effects were observed by Ku *et al.* (31) with an apparent strain threshold of 7%. We observed increases in UTS and E of constructs at 10% and 15% CD, with no differences between values at 10% and 15% CD.

In contrast, the collagen concentration was found to be greater than controls only at 15% CD, indicating that there is some difference in the cell response to 10% vs. 15% CD. This difference in cell response suggested that CD might also improve tensile mechanical properties by improving the functional quality of ECM. Picrosirius red stains for mature collagen fibers, which have been defined as thicker (32), more aligned (33) and more cross-linked (34). We found that CD and ICD constructs stained brighter, indicating more collagen maturation, compared with controls (Fig. 4), which likely contributed to their improved mechanical properties. Balguid *et al.* (34) correlated the modulus of tissue-engineered valve leaflets and native pig valve leaflets with collagen cross-linking, showing via Picrosirius red staining that constructs with higher modulus had stronger staining. Similarly in our case, the maturation observed in CD and ICD constructs by Picrosirius red staining also correlates with higher UTS and E than controls (Fig. 1). The Trichrome-stained sections also revealed that CD and ICD constructs exhibited stronger cell alignment in the circumferential direction compared with static controls. Qualitatively, the cell alignment correlates with maturation of the cell-produced collagen, also exhibiting strong circumferential alignment, as implied by the Picrosirius red stain. These findings are consistent with the cells exhibiting a contact guidance response to the aligned cell-produced collagen fibers, a phenomenon characterized in statically incubated constructs (35), but not in CD constructs.

We hypothesized that long-term CD may induce an adaptation response of the cells. Such an adaptive response to CD has been reported with osteoblasts (25, 26). However, analogous studies have not been reported in cardiovascular tissue engineering. To test this hypothesis, we conducted experiments with a time-averaged CD strain amplitude of 10% in increments from 5% to 15% in two or four equal time steps during 3 weeks of CD (Fig.

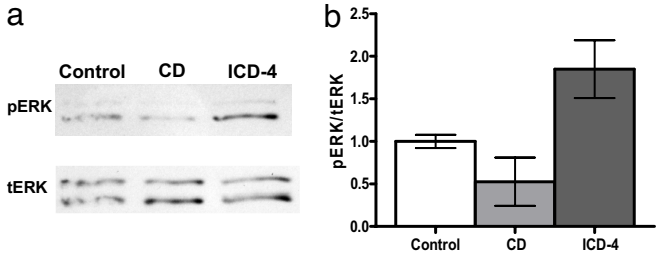

Fig. 5. Western blot for ERK 1/2 activation after CD. (*a*) Twenty micrograms of protein was analyzed by Western blot for levels of total (tERK) and Thr-202/Tyr-204 pERK 1/2. Protein was isolated from control, 10% CD, and ICD-4 constructs after 3 weeks of CD. Bands appear at 42/44 kDa. (*b*) Band intensity was determined by densitometry and expressed as the ratio of pERK and tERK, normalized to the control value. Ranges for two blots are shown.

1*a Inset*). UTS and E improved greatly with ICD-4 beyond what was achieved with CD (98% and 61% higher, respectively), attaining the values of 2.30 and 11.4 MPa, respectively. These values compare favorably with those of native cardiovascular tissues (30). UTS and E also differed among the 15% CD, ICD-2, and ICD-4 groups. These results are consistent with an adaptive behavior at CD that was partially overcome with ICD-2 and further overcome with the more frequent stimulus perturbation of ICD-4. It can be concluded that the adaptation time for the cell response leading to improvement in mechanical properties is smaller than 3–4 days, which was the duration of each strain amplitude in ICD-4.

A trend similar to the effect of CD on mechanical properties was found for collagen concentration. Moreover, the collagen concentration normalized by the cell concentration increased only in the case of ICD, consistent with ICD acting to mitigate a reduction in the rate of collagen deposited per cell resulting from adaptation to constant CD.

Experiments with HDF constructs showed results similar to PVIC constructs: ICD-4 again showed improvement in mechanical properties and collagen concentration beyond what was achieved with CD. These results demonstrate that the apparent adaptation response to CD is not restricted to a particular tissue cell type. A time-course study with HDF constructs also revealed that whereas the UTS and collagen content of controls progressively increased over 3 weeks, they dramatically increased during week 3 for the ICD constructs.

Consistent with the hypothesis that ICD mitigates adaptation to the stimulus presented by CD, a 255% increase in pERK was observed in ICD-4 vs. 10% CD constructs after 3 weeks of CD. Papakrivopoulou *et al.* (29) have shown that pERK elevation correlated with collagen expression in cardiac fibroblasts adhered to distensible membranes when subjected to CD, which is consistent with our results showing elevated pERK and increased collagen deposition per cell for HDF constructs subjected to ICD-4. Although our results are consistent with adaptation to CD, which is mitigated with ICD, it is recognized that there are other possible explanations for these results besides invoking adaptation. For example, if the collagen produced by the cells becomes increasingly less susceptible to degradation when stretched (36), the collagen concentration in the ICD constructs should be more than the 10% CD constructs, as is the case. Even if the beneficial effect of constant CD and ICD is directly connected to cell metabolism via ERK signaling, it is still unknown whether the mechanism is caused by cyclic mechanical strain of the cells or altered transport of biomolecules through the tissue during its transient compression (37). Regardless of the mechanism, the application of CD generally and ICD specifically can be used to improve mechanical and biochemical properties and structural organization of tissue-engineered tubular constructs, which has direct relevance to the fabrication of vascular and heart valve constructs using bioreactors that apply controlled stretching.

Materials and Methods

Cell Culture. PVICs were isolated from porcine aortic valve leaflets (generously donated by Experimental Surgical Services at the University of Minnesota) by a 30-min enzymatic digestion with 1 mg/ml collagenase and 0.5 mg/ml elastase. PVIC were cultured in DMEM/F12 culture medium (Gibco) supplemented with 10% FBS (HyClone), 100 units/ml penicillin, and 100 μg/ml streptomycin. Cells were incubated at 37°C in 100% humidity and 5% CO_2. Cells were passaged at 80–90% confluency and harvested for use from passages 5–8.

Neonatal HDFs (Clonetics) were maintained in DMEM/F12 supplemented with 10% FBS,100 units/ml penicillin, 100 μg/ml streptomycin, and 2.5 μg/ml amphotericin-β. Cells were passaged at 100% confluency and harvested for use from passages 7–9.

Tubular Construct Preparation and Culture. A cell-seeded fibrin gel was molded by mixing cells suspended in DMEM into a solution of bovine fibrinogen (Sigma) in 20 mM Hepes-buffered saline. A mixture of bovine thrombin (Sigma) and calcium chloride in DMEM was then added to the suspension. All components were at room temperature. For PVIC constructs, final concentrations were 3.3 mg/ml fibrinogen, 0.2 units/ml thrombin, 1.8 mM Ca^{2+}, and 500,000 cells/ml. For HDF constructs, final concentrations were 6.6 mg/ml fibrinogen, 0.4 units/ml thrombin, 3.6 mM Ca^{2+}, and 500,000 cells/ml. Suspensions were mixed well by trituration and injected into tubular molds comprised of a Teflon mandrel centered in a polypropylene casing.

The molds were then placed vertically in an incubator for 30 min. After gelation, the casing was removed and the constructs were placed horizontally in culture medium. PVIC constructs were cultured in 50:50 DMEM/F12 supplemented with 10% FBS, 100 units/ml penicillin, 100 μg/ml streptomycin, 1 ng/ml TGF-β, 2 μg/ml insulin, 50 μg/ml ascorbic acid, and 2 mg/ml ε-aminocaproic acid. HDF constructs were cultured in DMEM supplemented with 10% FBS, 100 units/ml penicillin, 100 μg/ml streptomycin, 2 μg/ml insulin, 50 μg/ml ascorbic acid, and 2.5 μg/ml amphotericin-β. Initially, the constructs had an internal diameter of 8 mm, a thickness of 3.8 mm, and a length of 12.5 mm. Constructs were cultured for 2 weeks, after which they were transferred to the CD bioreactor. This process allowed for cell-mediated fibrin compaction and initial ECM deposition so that the constructs could withstand transfer to the bioreactor.

CD Bioreactor. Constructs were transferred onto a distensible mandrel in a custom-built bioreactor as described (7). In brief, the distensible mandrel was a thin latex tube (Kent Elastomer). One end of the tube was closed with a polycarbonate stopper by using epoxy sealant, while the other end was connected to an in-house air line regulated by a pressure regulator. The frequency and duty of the air cycle were controlled by a solenoid valve connected downstream of the pressure regulator. Digital images were taken of the latex tube at different inlet air pressures, and a pressure–diameter correlation was recorded, which was used to set the maximum strain for each experiment. For all studies, a frequency of 0.5 Hz with 12.5% duty cycle was used, corresponding to a 0.25-s stretch time in a 2-s cycle period. For CD experiments, a strain amplitude of 2.5%, 5%, 10%, 15%, or 20% was applied to constructs for 3 weeks. For ICD experiments, the strain amplitude was incremented from 5% to 15% in two and four equal time steps over 3 weeks (Fig. 1*a Inset*). Seventy percent of the medium in the CD bioreactor was changed three times per week.

After harvest, each construct was divided into three sections of equal length for tensile testing followed by biochemical analysis, DNA quantification, and histology or protein extraction.

Uniaxial Tensile Testing. A one-third strip of a construct was tested for uniaxial properties in the circumferential direction. The thickness was measured by using a 50-g force probe attached to a displacement transducer. Tissue strips were then placed in compressive grips, attached to the actuator arm and load cell of a Microbionix (MTS Systems), and straightened with a load of 0.005 N. This position was used as the reference length of the strip. After six cycles of 0–10% strain at 2 mm/min, constructs were stretched to failure. True strain was calculated based on the change in length of the tissue over time. The stress was calculated as force divided by the initial cross-sectional area. Young's modulus (E) was determined by linear regression of the stress-strain curve.

Histology. Constructs for histology were fixed in 4% paraformaldehyde, infiltrated with a solution of 30% sucrose and 5% DMSO, frozen in OCT (Tissue-Tek), and sectioned into 9-μm cross-sections. Sections were stained with Lillie's Trichrome and Picrosirius red. Images were taken at ×10 with a color CD camera. For Picrosirius red, images were taken with the samples placed between crossed plane polarizers.

Collagen and Cell Quantification. Collagen content was quantified by the hydroxyproline assay (19). Sample volume was calculated by using the measured length, width, and thickness of the strips. Collagen concentrations were calculated as the amount per unit volume in each sample, assuming 7.7 mg of collagen per mg of hydroxyproline.

DNA content was quantified with a modified Hoechst assay (19). Cell numbers were obtained from DNA contents assuming 7.6 pg of DNA per cell. Cell concentrations were calculated as the number of cells per unit volume by using the dimensions of the strip.

Protein Extraction. For each condition, tissue was pooled from two constructs and rinsed with PBS. The tissue was then disrupted by sonication in ice-cold lysis buffer [25 mM Tris (pH 7.4), 225 mM NaCl, 25 mM NaF, 5% glycerol, 0.5% Nonidet P-40, 0.025% sodium deoxycholate, 1 mM EDTA, 2 mM $NaVO_4$, 1 μg/ml aprotinin, pepstatin, and leupeptin]. The soluble lysate was isolated by

centrifugation, and the protein concentration was determined by BCA assay (Pierce).

Western Blot. For each sample, 20 μg of total protein was boiled in reducing sample buffer and separated by SDS/PAGE. Protein was transferred to nitrocellulose (Whatman) by using wet transfer buffer (10% methanol, 2.2 g/liter 3-(cyclohexylamino)-1-propanesulfonic acid, pH 11). The blot was incubated in blocking solution (5% dry milk, 0.1% Tween-20 in PBS) for 1 h and then incubated with primary rabbit polyclonal phospho-ERK antibody (*p*-Thr-202/*p*-Tyr-204; Calbiochem; 1:2,500) overnight at 4°C. The blot was then probed with HRP-conjugated secondary anti-rabbit IgG (Amersham) at a dilution of 1:10,000 and developed by using enhanced chemiluminescence. The blot was then stripped of antibodies by using Restore Plus (Pierce) and reprobed with rabbit polyclonal ERK1/2 antibody (Calbiochem; 1:2,500). The pERK-to-total-ERK ratio was determined by densitometry of scanned autoradiograms.

Statistics. For each group of constructs, a subset was randomly chosen as the paired static controls, which were mounted in the bioreactor but not subjected to CD ($n = 5–8$). The remaining constructs were subjected to CD as described ($n = 5–8$). The mean of the measurements obtained from the static controls were used to normalize the paired CD constructs so that results could be compared from different experiments, where variability in the control values occurred. The controls value of $1 \pm$ SD in Figs. 1 and 2 represents the mean of all normalized control values from all experiments. Statistical difference between groups was determined by one-way ANOVA using SPSS software for Windows. Levene's test was used for homogeneity of population variances among groups. If the test was significant ($P < 0.05$), post hoc analysis was done by using the Games-Howell procedure, which does not assume equal variance between groups. Otherwise the Schieffe method was used. In all cases where the error bars (plus or minus standard deviation) are nonoverlapping, the differences are significant; hence, for clarity, no symbols are used. In cases where error bars are overlapping and the difference is statistically significant, paired symbols are used to indicate the difference. Any reference to a difference in *Results* and *Discussion* implies statistical significance at the level $P < 0.05$.

ACKNOWLEDGMENTS. We thank Ricky Chow, Naomi Ferguson, Katie Hill, and Stephen Stephens for technical assistance. This work was supported by National Institutes of Health Grants BRP HL71538 and HL083880 (to R.T.T.).

1. Butler DL, Goldstein SA, Guilak F (2000) Functional tissue engineering: The role of biomechanics. *J Biomech Eng* 122:570–575.
2. Freed LE, *et al.* (2006) Advanced tools for tissue engineering: Scaffolds, bioreactors, and signaling. *Tissue Eng* 12:3285–3305.
3. Jeong SI, *et al.* (2005) Mechano-active tissue engineering of vascular smooth muscle using pulsatile perfusion bioreactors and elastic PLCL scaffolds. *Biomaterials* 26:1405–1411.
4. Solan A, Mitchell S, Moses M, Niklason L (2003) Effect of pulse rate on collagen deposition in the tissue-engineered blood vessel. *Tissue Eng* 9:579–586.
5. Hahn MS, *et al.* (2007) Physiologic pulsatile flow bioreactor conditioning of poly(ethylene glycol)-based tissue engineered vascular grafts. *Ann Biomed Eng* 35:190–200.
6. Seliktar D, Nerem RM, Galis ZS (2003) Mechanical strain-stimulated remodeling of tissue-engineered blood vessel constructs. *Tissue Eng* 9:657–666.
7. Isenberg BC, Tranquillo RT (2003) Long-term cyclic distention enhances the mechanical properties of collagen-based media equivalents. *Ann Biomed Eng* 31:937–949.
8. Cummings CL, Gawlitta D, Nerem RM, Stegemann JP (2004) Properties of engineered vascular constructs made from collagen, fibrin, and collagen-fibrin mixtures. *Biomaterials* 25:3699–3706.
9. Seliktar D, Black RA, Vito RP, Nerem RM (2000) Dynamic mechanical conditioning of collagen-gel blood vessel constructs induces remodeling *in vitro*. *Ann Biomed Eng* 28:351–362.
10. Niklason LE, *et al.* (1999) Functional arteries grown *in vitro*. *Science* 284:489–493.
11. Kim BS, Nikolovski J, Bonadio J, Mooney DJ (1999) Cyclic mechanical strain regulates the development of engineered smooth muscle tissue. *Nat Biotechnol* 17:979–983.
12. Isenberg BC, Williams C, Tranquillo RT (2006) Small-diameter artificial arteries engineered *in vitro*. *Circ Res* 98:25–35.
13. Hoerstrup SP, *et al.* (2000) New pulsatile bioreactor for *in vitro* formation of tissue engineered heart valves. *Tissue Eng* 6:75–79.
14. Hildebrand DK, Wu ZJ, Mayer JE, Jr, Sacks MS (2004) Design and hydrodynamic evaluation of a novel pulsatile bioreactor for biologically active heart valves. *Ann Biomed Eng* 32:1039–1049.
15. Mol A, *et al.* (2005) Tissue engineering of human heart valve leaflets: A novel bioreactor for a strain-based conditioning approach. *Ann Biomed Eng* 33:1778–1788.
16. Chester AH, Taylor PM (2007) Molecular and functional characteristics of heart-valve interstitial cells. *Philos Trans R Soc London Ser B* 362:1437–1443.
17. Hoerstrup SP, *et al.* (2000) Functional living trileaflet heart valves grown *in vitro*. *Circulation* 102:III-44–III-49.
18. Grassl ED, Oegema TR, Tranquillo RT (2002) Fibrin as an alternative biopolymer to type-I collagen for the fabrication of a media equivalent. *J Biomed Mater Res* 60:607–612.
19. Robinson PS, *et al.* (2007) Functional tissue-engineered valves from cell-remodeled fibrin with commissural alignment of cell-produced collagen. *Tissue Eng* 14:83–95.
20. Isenberg BC, Williams C, Tranquillo RT (2006) Endothelialization and flow conditioning of fibrin-based media equivalents. *Ann Biomed Eng* 34:971–985.
21. Williams C, Johnson SL, Robinson PS, Tranquillo RT (2006) Cell sourcing and culture conditions for fibrin-based valve constructs. *Tissue Eng* 12:1489–1502.
22. Grinnell F, Ho CH (2002) Transforming growth factor β stimulates fibroblast-collagen matrix contraction by different mechanisms in mechanically loaded and unloaded matrices. *Exp Cell Res* 273:248–255.
23. Turner CH, Robling AG, Duncan RL, Burr DB (2002) Do bone cells behave like a neuronal network? *Calcified Tissue Int* 70:435–442.
24. Li YS, Haga JH, Chien S (2005) Molecular basis of the effects of shear stress on vascular endothelial cells. *J Biomech* 38:1949–1971.
25. Turner CH (1998) Three rules for bone adaptation to mechanical stimuli. *Bone* 23:399–407.
26. Schriefer JL, *et al.* (2005) Cellular accommodation and the response of bone to mechanical loading. *J Biomech* 38:1838–1845.
27. Kim CH, *et al.* (2003) Trabecular bone response to mechanical and parathyroid hormone stimulation: The role of mechanical microenvironment. *J Bone Miner Res* 18:2116–2125.
28. Tang LL, Wang YL, Pan J, Cai SX (2004) The effect of step-wise increased stretching on rat calvarial osteoblast collagen production. *J Biomech* 37:157–161.
29. Papakrivopoulou J, Lindahl GE, Bishop JE, Laurent GJ (2004) Differential roles of extracellular signal-regulated kinase 1/2 and p38MAPK in mechanical load-induced procollagen α1(I) gene expression in cardiac fibroblasts. *Cardiovasc Res* 61:736–744.
30. Lo D, Vesely I (1995) Biaxial strain analysis of the porcine aortic valve. *Ann Thorac Surg* 60:S374–S378.
31. Ku CH, *et al.* (2006) Collagen synthesis by mesenchymal stem cells and aortic valve interstitial cells in response to mechanical stretch. *Cardiovasc Res* 71:548–556.
32. Dayan D, *et al.* (1989) Are the polarization colors of picrosirius red-stained collagen determined only by the diameter of the fibers? *Histochemistry* 93:27–29.
33. Junqueira LC, Montes GS, Sanchez EM (1982) The influence of tissue section thickness on the study of collagen by the Picrosirius-polarization method. *Histochemistry* 74:153–156.
34. Balguid A, *et al.* (2007) The role of collagen cross-links in biomechanical behavior of human aortic heart valve leaflets: Relevance for tissue engineering. *Tissue Eng* 13:1501–1511.
35. Grassl ED, Oegema TR, Tranquillo RT (2003) A fibrin-based arterial media equivalent. *J Biomed Mater Res A* 66:550–561.
36. Ruberti JW, Hallab NJ (2005) Strain-controlled enzymatic cleavage of collagen in loaded matrix. *Biochem Biophys Res Commun* 336:483–489.
37. Chahine NO, *et al.* (2008) Effect of dynamic loading on the transport of solutes into agarose hydrogels. *Biophys J*, in press.